DTIC FILE COPY ②

ICASE

BOUNDARY SHAPE IDENTIFICATION PROBLEMS
IN TWO-DIMENSIONAL DOMAINS RELATED TO
THERMAL TESTING OF MATERIALS

AD-A194 917

DTIC
S ELECTE D
JUN 0 7 1988
C&D

H. T. Banks

Fumio Kojima

NASA

National Aeronautics and
Space Administration

Langley Research Center
Hampton, Virginia 23665

BOUNDARY SHAPE IDENTIFICATION PROBLEMS IN TWO-DIMENSIONAL DOMAINS RELATED TO THERMAL TESTING OF MATERIALS

H. T. Banks
Center for Control Sciences
Division of Applied Mathematics
Brown University
Providence, RI 02912

Fumio Kojima
Institute for Computer Applications in Science and Engineering
NASA Langley Research Center
Hampton, VA 23665

Abstract

This paper is concerned with the identification of the geometrical structure of the system boundary for a two-dimensional diffusion system. The domain identification problem treated here is converted into an optimization problem based on a fit-to-data criterion and theoretical convergence results for approximate identification techniques are discussed. Results of numerical experiments to demonstrate the efficacy of the theoretical ideas are reported.

I. INTRODUCTION

' Domain identification problems are important in the design of engineering systems and frequently such problems are treated as a branch of the calculus of variations which involves nonlinear optimization techniques, optimal control theory, partial differential equations (elliptic, parabolic, hyperbolic, etc.) and related numerical methods. Domain identification for elliptic systems has been studied theoretically and numerically by many authors (see e.g., [5],[7],[10],[13]). For parabolic systems, a couple of numerical methods for identifying the domain or boundary have been investigated in [14],[15]. Until recently, most investigations concentrated on the "optimal shape design problem" which is motivated by numerous applications to structural, engine, airplane, ship designs, etc. (see [10] and the references therein). In this paper, our concern for domain identification is motivated by an application that is different from these shape design problems. However, as we shall see, the resulting theoretical aspects are closely related. Recently, associated with the use of fiber reinforced composite materials for aerospace structures, there is growing interest in the detection and characterization of large structural flaws which may not be detectable by visual inspection. One recent effort has focused on non-destructive evaluation methods (NDE) based on the measurement of thermal diffusivity in composite materials (see e.g., [8]). Motivated by these problems, we consider the domain identification for parabolic systems. .

To explain our approach, we restrict our attention to a 2-D domain identification problem. We consider the bounded domain $G(q)$ in two-dimensional Euclidean space as follows:

$$G(q) = \{(x_1, x_2) | 0 < x_1 < 1, \ 0 < x_2 < r(x_1, q)\}$$

where $x_1 \rightarrow r(x_1, q)$ is some parameterized real function which is assumed to characterize the unknown part of the boundary and q is a constant parameterization vector to be identified among values in a given compact admissible parameter set Q. As depicted in

1
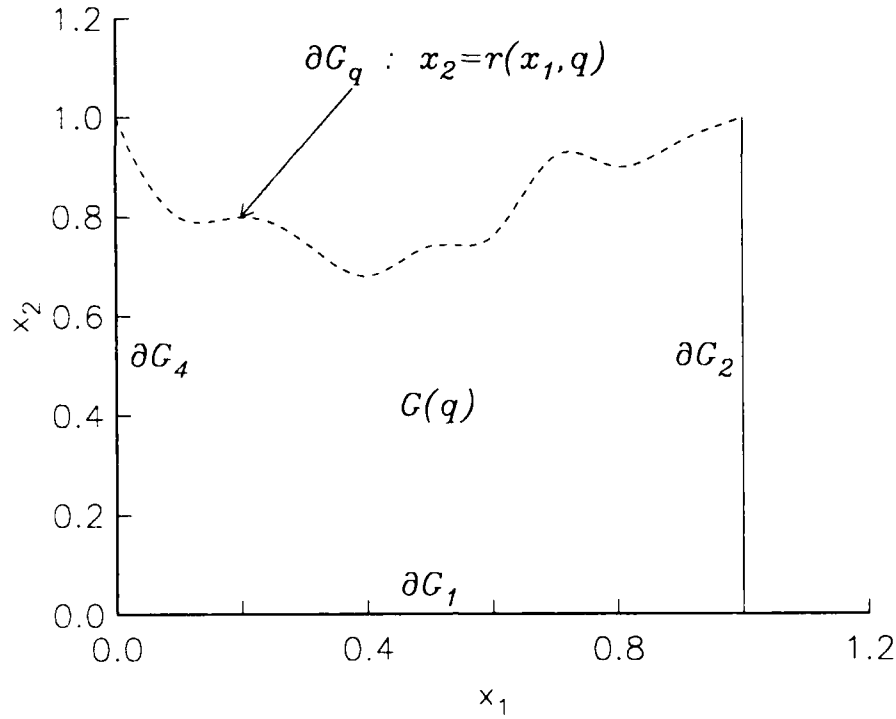
Fig. 1.1. The spatial domain G and its boundary ∂G_1, ∂G_2, ∂G_q, ∂G_4.

Fig. 1.1, we assume the boundary of $G(q)$ consists of the following components:

$$\partial G_1 = \{x = (x_1, x_2) | 0 < x_1 < 1,\ x_2 = 0\}$$

$$\partial G_2 = \{x = (x_1, x_2) | x_1 = 1,\ 0 < x_2 < \ell\}$$

$$\partial G_q = \{x = (x_1, x_2) | 0 < x_1 < 1,\ x_2 = r(x_1, q)\}$$

$$\partial G_4 = \{x = (x_1, x_2) | x_1 = 0,\ 0 < x_2 < \ell\}$$

The measurement system is described by the following 2-D diffusion equation:

$$\frac{\partial u(t, x)}{\partial t} - c_1 \Delta u(t, x) + c_0 u(t, x) = 0 \qquad \text{in } T \times G(q) \tag{1.1a}$$

with the initial and boundary conditions,

$$u(0, x) = \overline{u}_0(x) \qquad \text{on } G(q) \tag{1.1b}$$

2

$$-c_1\frac{\partial u}{\partial x_2} + h(u - f) = 0 \qquad \text{on} \quad T \times \partial G_1 \qquad (1.1c)$$

$$c_1\frac{\partial u}{\partial x_1} + hu = 0 \qquad \text{on} \quad T \times \partial G_2 \qquad (1.1d)$$

$$\frac{\partial u}{\partial n} = 0 \qquad \text{on} \quad T \times \partial G_q \qquad (1.1e)$$

$$-c_1\frac{\partial u}{\partial x_1} + hu = 0 \qquad \text{on} \quad T \times \partial G_4 \qquad (1.1f)$$

where c_1, c_0 and h are thermal diffusivity, radiation coefficient and heat transfer coefficient, respectively, which are given constants, and where T denotes the time interval $(0, t_f)$ during which the process is observed. In the above system, f is the known boundary input defined on $T \times \partial G_1$ and $\overline{u}_0$ is the given initial function defined on Ω where Ω is a known bounded domain in R^2 such that $\Omega \supset G(q)$ for any $q \epsilon Q$. The system output is assumed to be on a subset Σ of the boundary ∂G_1, and mathematically, the observation is taken as

$$y(t, x, q) = u(t, x_1, 0, q) \qquad (t, x)\epsilon T \times \Sigma. \qquad (1.2)$$

From a physical point of view, the system state $u = u(t, x)$ represents the temperature distribution at time t at location $x = (x_1, x_2)$ and, the boundary input f and the output y correspond, respectively, to the thermal source (for example, by a laser beam) and the observation of the temperature distribution at the surface of the material (e.g., by an infrared imager) (see [8] for more details). Thus, the search for structural flaws in materials may be formulated as an inverse problem for a heat diffusion system. The problem treated here is that of identifying, from input and output data $\{f, \overline{u}_0, y\}$ on $(T \times \partial G_1) \times G \times (T \times \Sigma)$, the constant parameter vector q in Q determining the geometrical structure of the boundary ∂G_q.

In Section 2, we formulate this problem in an abstract setting in a Hilbert space. In Section 3, for computational purposes, we approximate the Hilbert space by finite dimensional subspaces and we discuss the convergence analysis for the approximate identification problems. In Section 4, a practical optimization technique based on a finite element approach is outlined. Some numerical results for a simple example are given in Section 5.

3

II. PROBLEM FORMULATION AND BASIC ASSUMPTIONS

For the discussions here, we restrict the geometrical structure of the boundary ∂G_q by imposing the following hypotheses:

(H-0) The admissible parameter set Q is a compact subset of R^n;

(H-1) For each $q \epsilon Q$, we have $r(q) \epsilon W_\infty^1(0,1)$;

(H-2) For each $q \epsilon Q$, we have $r(0,q) = r(1,q) = \ell$;

(H-3) There are constants β_1 and β_2 satisfying $0 < \beta_1 < \ell < \beta_2 < \infty$ such that, for $q \epsilon Q$, we have

$$\beta_1 \leq r(\xi,q) \leq \beta_2 \qquad \text{a.e. in} \qquad (0,1);$$

and

(H-4) There exists a constant M such that

$$|r(\xi,q) - r(\xi,\tilde{q})|_{1,\infty} \leq M|q - \tilde{q}| \qquad \text{for} \qquad q, \tilde{q} \epsilon Q, \xi \epsilon [0,1],$$

where $|\cdot|_{1,\infty}$ denotes the norm of $W_\infty^1(0,1)$.

We make the following assumptions for the class of system inputs:

(H-5) $$\overline{u}_0 \epsilon L^2(\Omega);$$

and

(H-6) $$f \epsilon L^2(T; L^2(0,1)).$$

It follows from results in ([9], Ch. 3) that, under the hypotheses (H-1)-(H-3), (H-5), and (H-6), for each fixed $q \epsilon Q$, there exists for (1.1) a unique solution u in $L^2(T; H^1(G(q)))$. Following standard procedures in optimal shape design techniques ([10], Ch. 8, p. 125), we introduce the affine mapping

$$(z_1, z_2) = \mathcal{T}(q)(x_1, x_2)$$

4

given by

$$z_1 = x_1$$

$$z_2 = \frac{\ell x_2}{r(x_1, q)}.$$

Note that this is equivalent to $x_1 = z_1, x_2 = r(z_1, q)z_2/\ell$. Under this coordinate change, the system domain $G(q)$ is transformed into the fixed domain $\tilde{G}$

$$G(q) \to \tilde{G} = (0, 1) \times (0, \ell)$$

which is independent of the parameter q. Using this coordinate transformation, we obtain the system state $\tilde{u}$ given by

$$\tilde{u}(t, z) = u(t) \circ \mathcal{T}^{-1}(q) = u(t, x_1(z_1),\ x_2(z_1, z_2));$$

this transformed state then satisfies the system equation

$$\frac{\partial \tilde{u}(t, z)}{\partial t} - \sum_{i, j \leq 2} \frac{\partial}{\partial z_i} \left(a_{ij}(z) \frac{\partial \tilde{u}(t, z)}{\partial z_j} \right) + \sum_{j \leq 2} b_j(z) \frac{\partial \tilde{u}(t, z)}{\partial z_j} + c_0 \tilde{u}(t, z) = 0 \qquad \text{in} \qquad T \times \tilde{G} \tag{2.1a}$$

with

$$\tilde{u}(0, z) = \bar{u}_0(z) \circ \mathcal{T}^{-1}(q) \qquad \text{on} \qquad \tilde{G} \tag{2.1b}$$

$$-\frac{c_1 \ell}{r(z_1, q)} \frac{\partial \tilde{u}}{\partial z_2} + h(\tilde{u} - f) = 0 \qquad \text{on} \qquad T \times \partial G_1 \tag{2.1c}$$

$$c_1 \frac{\partial \tilde{u}}{\partial z_1} - \frac{c_1}{\ell} z_2 r'(1, q) \frac{\partial \tilde{u}}{\partial z_2} + h\tilde{u} = 0 \qquad \text{on} \qquad T \times \partial G_2 \tag{2.1d}$$

$$r'(z_1, q) \frac{\partial \tilde{u}}{\partial z_1} - \frac{\ell}{r(z_1, q)} \left[\{r'(z_1, q)\}^2 + 1 \right] \frac{\partial \tilde{u}}{\partial z_2} = 0 \qquad \text{on} \qquad T \times \partial G_3 \tag{2.1e}$$

$$-c_1 \frac{\partial \tilde{u}}{\partial z_1} + \frac{c_1}{\ell} z_2 r'(0, q) \frac{\partial \tilde{u}}{\partial z_2} + h\tilde{u} = 0 \qquad \text{on} \qquad T \times \partial G_4. \tag{2.1f}$$

5

In this system the coefficients are given by

$$a_{11} := c_1 \tag{2.2}$$

$$a_{12}(z) = a_{21}(z) := -\frac{c_1 r'(z_1, q) z_2}{r(z_1, q)} \tag{2.3}$$

$$a_{22}(z) := \frac{c_1}{\{r(z_1, q)\}^2} \left[\{r'(z_1, q)\}^2 z_2^2 + \ell^2 \right] \tag{2.4}$$

$$b_1(z) := -\frac{c_1 r'(z_1, q)}{r(z_1, q)} \tag{2.5}$$

$$b_2(z) := \frac{c_1 \{r'(z_1, q)\}^2 z_2}{\{r(z_1, q)\}^2} \tag{2.6}$$

where r' denotes dr/dz_1, while ∂G_q has been mapped into

$$\partial G_3 = \{z = (z_1, z_2) | 0 < z_1 < 1, \ z_2 = \ell\}.$$

If we consider a variational formulation similar to that in [2],[9], the system dynamics can be described by the variational form:

$$< \frac{d\tilde{u}(t)}{dt}, \phi > + \sigma(q)(\tilde{u}(t), \phi) = L(t, q)(\phi) \qquad \text{for} \qquad \phi \epsilon H^1(\tilde{G})$$

$$\tag{2.7}$$

$$\tilde{u}(0) = \overline{u}_0 \circ \mathcal{T}^{-1}(q)$$

where the bracket $< \cdot, \cdot >$ denotes the scalar product in $L^2(\tilde{G})$ and where $\sigma(q)(\cdot, \cdot)$ and $L(q)(\cdot)$ denote, respectively, a sesquilinear form on $H^1(\tilde{G}) \times H^1(\tilde{G})$ and a linear functional on $H^1(\tilde{G})$. Explicitly, $\sigma(q)(\cdot, \cdot)$ and $L(q)(\cdot)$ are given by for $\phi, \psi \epsilon H^1(\tilde{G})$ by

$$\sigma(q)(\phi, \psi) := \int\int_{\tilde{G}} [\sum_{i,j \leq 2} a_{ij}(z) \frac{\partial \phi}{\partial z_j} \frac{\partial \psi}{\partial z_i} + \sum_{j \leq 2} b_j(z) \frac{\partial \phi}{\partial z_j} \psi + c_0 \phi \psi] dz + \int_0^1 \frac{\ell h}{r(z_1, q)} [\phi \psi]_{\partial G_1} dz_1$$

$$\tag{2.8}$$

$$+ \int_0^\ell h [\phi \psi]_{\partial G_2 \cup \partial G_4} dz_2,$$

$$L(t, q)(\phi) := \int_0^1 \frac{\ell h}{r(z_1, q)} f(t, z_1) [\phi]_{\partial G_1} dz_1, \tag{2.9}$$

6

respectively. With some tedious calculations, one can readily establish the following useful conditions on the sesquilinear form σ.

Theorem 1: *Let $|\cdot|_V$ and $|\cdot|_H$ denote the norms in the Hilbert spaces $V = H^1(\tilde{G})$ and $H = L^2(\tilde{G})$. Then, under the hypotheses (H-0) to (H-4), the sesquilinear forms $\sigma(q)(\cdot,\cdot)$ satisfy the following inequalities: There exist positive constants $k_1, \lambda, k_2,$ and k_3 such that for $\phi, \psi \epsilon V$ we have*

$$\sigma(q)(\phi,\phi) \geq k_1|\phi|_V^2 - \lambda|\phi|_H^2 \tag{2.10}$$

$$\sigma(q)(\phi,\psi) \leq k_2|\phi|_V|\psi|_V \tag{2.11}$$

$$|\sigma(q)(\phi,\psi) - \sigma(\tilde{q})(\phi,\psi)| \leq k_3|q - \tilde{q}||\phi|_V|\psi|_V \qquad \text{for all} \qquad q, \tilde{q} \epsilon Q. \tag{2.12}$$

Proof: We wish to show first that the sesquilinear form σ is coercive. From (2.2)-(2.4) and (2.8), the principal part of the differential operator becomes

$$\sum_{i,j \leq 2} a_{ij}(z,q)\xi_i\xi_j = c_1\xi_1^2 - \frac{2c_1 r'(z_1,q)z_2}{r(z_1,q)}\xi_1\xi_2 + \frac{c_1}{\{r(z_1,q)\}^2}[\{r'(z_1,q)\}^2 z_2^2 + \ell^2]\xi_2^2$$

$$\text{for} \qquad (\xi_1,\xi_2) \epsilon R^2. \tag{2.13}$$

By simple calculations and from (H-3), we have

$$\sum_{i,j \leq 2} a_{i,j}(z,q)\xi_i\xi_j \geq \frac{c_1\ell^2}{2}\left(\frac{|\xi_1|^2}{\{r'(z_1,q)\}^2 z_2^2 + \ell^2} + \frac{|\xi_2|^2}{\{r(z_1,q)\}^2}\right) \geq K_1(|\xi_1|^2 + |\xi_2|^2) \tag{2.14}$$

where

$$K_1 = \frac{c_1\ell^2}{2\beta_2^2}.$$

This means the operator is strongly elliptic. For the coefficients $b_j(z,q)(j = 1,2)$, from (2.5) and (2.6), it follows that

$$|b_1(z,q)| \leq \frac{c_1}{\beta_1} \sup_{z_1\epsilon[0,1]} |r'(z_1,q)| \tag{2.15}$$

$$|b_2(z,q)| \leq \frac{c_1\ell}{\beta_1^2} \sup_{z_1\epsilon[0,1]} |r'(z_1,q)|^2 \tag{2.16}$$

7

respectively. We note that, from (H-0) to (H-4),

$$\sup_{z_1 \in [0,1]} |r'(z,q)| < R \tag{2.17}$$

where R is some constant independent of q. Hence, we obtain

$$|b_j(z,q)| \le K_2 < \infty \qquad \text{for} \qquad j = 1, 2, \tag{2.18}$$

where (assuming $R > 1$)

$$K_2 = \frac{c_1 \ell R^2}{\beta_1^2}. \tag{2.19}$$

For the last two boundary integrals in (2.8), by virtue of (H-3), the following inequality holds:

$$\int_0^1 \frac{\ell h}{r(z_1,q)} [\phi^2]_{\partial G_1} dz_1 + \int_0^\ell h [\phi^2]_{\partial G_2 \cup \partial G_4} dz_2 \ge h \int_{\partial \overline{G}} [\phi^2]_{\partial \overline{G}} ds \tag{2.20}$$

where ds denotes a line element on $\partial \overline{G}$ and $\partial \overline{G} = \partial G_1 \cup \partial G_2 \cup \partial G_4$. From (2.14), (2.18), and (2.20), we can derive the coercivity property of the sesquilinear form. Namely, the sesquilinear form satisfies

$$
\begin{aligned}
\sigma(q)(\phi,\phi) &\ge K_1 \int\int_{\tilde{G}} \sum_{i \le 2} |\frac{\partial \phi}{\partial z_i}|^2 dz - K_2 \int\int_{\tilde{G}} \sum_{i \le 2} |\frac{\partial \phi}{\partial z_i}||\phi| dz \\
&\quad + h \int_{\partial \overline{G}} [\phi^2]_{\partial \overline{G}} ds \\
&\ge \frac{K_1}{4} \int\int_{\tilde{G}} \sum_{i \le 2} |\frac{\partial \phi}{\partial z_i}|^2 dz - \frac{K_2^2}{K_1} \int\int_{\tilde{G}} |\phi|^2 dz \\
&\quad + K_3 \left(\int\int_{\tilde{G}} \sum_{i \le 2} |\frac{\partial \phi}{\partial z_i}|^2 dz + \int_{\partial \overline{G}} [\phi^2]_{\partial \overline{G}} ds \right)
\end{aligned} \tag{2.21}
$$

where

$$K_3 = min \left(\frac{c_1 \ell}{4 \beta_2^2}, h \right).$$

Friedrich's second inequality ([1], p. 124) asserts that if $\partial \overline{G}$ is a nontrivial subset of $\partial \tilde{G}$, then there exists a positive constant α such that

$$\int\int_{\tilde{G}} \sum_{i \le 2} |\frac{\partial \phi}{\partial z_i}|^2 dz + \int_{\partial \overline{G}} [\phi^2]_{\partial \overline{G}} ds \ge \alpha(\tilde{G}) |\psi|_V^2. \tag{2.22}$$

8

By applying this to the last parenthesis of (2.21), we can conclude that

$$\sigma(q)(\phi,\phi) \geq K_4|\phi|_V^2 - K_5|\phi|_H^2, \tag{2.23}$$

where

$$K_4 = \frac{K_1}{4} + K_3\alpha(\tilde{G}), \qquad K_5 = \frac{K_2^2}{K_1} + \frac{K_1}{4}$$

respectively.

To prove the boundedness of $\sigma(q)$, we note that

$$|\sigma(q)(\phi,\psi)| \leq |\sum_{i,j\leq 2} \int\int_{\tilde{G}} a_{ij}(z,q)\frac{\partial\phi}{\partial z_j}\frac{\partial\phi}{\partial z_i}dz|$$

$$+|\sum_{j\leq 2}\int\int_{\tilde{G}} b_j(z,q)\frac{\partial\phi}{\partial z_j}\psi dz| + |\int\int_{\tilde{G}} c_0\phi\psi dz| \tag{2.24}$$

$$+|\int_0^1 \frac{\ell h}{r(z_1,q)}[\phi\psi]_{\partial G_1}dz_1 + \int_0^\ell h[\phi\psi]_{\partial G_2\cup\partial G_4}dz_2|.$$

The first three integrals of RHS in (2.24) satisfy

$$|\sum_{i,j\leq 2}\int\int_{\tilde{G}} a_{ij}(z,q)\frac{\partial\phi}{\partial z_j}\frac{\partial\psi}{\partial z_i}dz| \leq 4 \sup_{\substack{i,j\leq 2\\ z\in[0,1]\times[0,\ell]}} |a_{ij}(z,q)| \, |\phi|_V|\psi|_V \tag{2.25}$$

$$|\sum_{j\leq 2}\int\int_{\tilde{G}} b_j(z,q)\frac{\partial\phi}{\partial z_j}\psi dz| \leq 2 \sup_{\substack{j\leq 2\\ z\in[0,1]\times[0,\ell]}} |b_j(z,q)| \, |\phi|_V|\psi|_V \tag{2.26}$$

$$|\int\int_{\tilde{G}} c_0\phi\psi dz| \leq c_0|\phi|_V|\psi|_V, \tag{2.27}$$

respectively. From (2.2) to (2.4), it follows that, under hypotheses (H-1) and (H-3) (see (2.17)),

$$\sup_{\substack{i,j\leq 2\\ z\in[0,1]\times[0,\ell]}} |a_{ij}(z,q)| \leq K_6 < \infty \tag{2.28}$$

where

$$K_6 = \frac{c_1\ell^2}{\beta_1^2}(R^2 + 1).$$

From (2.18) and (2.25)-(2.28), we have

$$|\sigma(q)(\phi,\psi)| \leq (4K_6 + 2K_2 + c_0)|\phi|_V|\psi|_V + |\int_0^1 \frac{\ell h}{r(z_1,q)}[\phi\psi]_{\partial G_1}dz_1 + \int_0^\ell h[\phi\psi]_{\partial G_2\cup\partial G_4}dz_2|$$

$$\tag{2.29}$$

9

Furthermore, the boundary integral term satisfies

$$|\int_0^1 \frac{\ell h}{r(z_1,q)}[\phi\psi]_{\partial G_1}dz_1 + \int_0^\ell h[\phi\psi]_{\partial G_2 \cup \partial G_4}dz_2| \leq K_7|\phi|_V|\psi|_V \qquad (2.30)$$

which follows from the trace inequality ([1], p. 124)

$$\int_{\partial \tilde{G}}[\phi^2]_{\partial \tilde{G}}ds \leq \gamma(\tilde{G})|\phi|_V^2, \qquad (2.31)$$

where

$$K_7 = \frac{h\ell\gamma(\tilde{G})}{\beta_1}.$$

Consequently, we can prove the boundedness property of $\sigma(q)(\cdot,\cdot)$.

To establish the continuity property, we note that, for any q and $\tilde{q}\epsilon Q$,

$$|\sigma(q)(\phi,\psi) - \sigma(\tilde{q})(\phi,\psi)|$$

$$\leq |\int\int_{\tilde{G}}\sum_{i,j\leq 2}(a_{ij}(q) - a_{ij}(\tilde{q}))\frac{\partial\phi}{\partial z_j}\frac{\partial\psi}{\partial z_i}dz|$$

$$+|\int\int_{\tilde{G}}\sum_{j\leq 2}(b_j(q) - b_j(\tilde{q}))\frac{\partial\phi}{\partial z_j}\psi dz| \qquad (2.32)$$

$$+|\int_0^1 \ell h\left(\frac{1}{r(q)} - \frac{1}{r(\tilde{q})}\right)[\phi\psi]_{\partial G_1}dz_1|$$

$$\leq \int\int_{\tilde{G}}|a_{12}(q) - a_{12}(\tilde{q})|\{|\frac{\partial\phi}{\partial z_2}|\,|\frac{\partial\psi}{\partial z_1}| + |\frac{\partial\phi}{\partial z_1}|\,|\frac{\partial\psi}{\partial z_2}|\}dz$$

$$+\int\int_{\tilde{G}}|a_{22}(q) - a_{22}(\tilde{q})|\,|\frac{\partial\phi}{\partial z_2}|\,|\frac{\partial\phi}{\partial z_2}|dz$$

$$+\int\int_{\tilde{G}}|b_1(q) - b_1(\tilde{q})|\,|\frac{\partial\phi}{\partial z_1}|\,|\psi|dz + \int\int_{\tilde{G}}|b_2(q) - b_2(\tilde{q})|\,|\frac{\partial\phi}{\partial z_2}|\,|\psi|dz$$

$$+\int_0^1 \ell h|\frac{1}{r(q)} - \frac{1}{r(\tilde{q})}|\,|[\phi\psi]_{\partial G_1}|dz_1.$$

Under the hypotheses (H-1) and (H-3), we argue that

$$|a_{12}(q) - a_{12}(\tilde{q})| \leq \frac{c_1\ell}{\beta_1}max(\frac{R}{\beta_1},1)|r(q) - r(\tilde{q})|_{1,\infty}$$

$$|a_{22}(q) - a_{22}(\tilde{q})| \leq \frac{2c_1\ell^2 R}{\beta_1^2}max(\frac{2R\beta_2}{\beta_1^2},1)|r(q) - r(\tilde{q})|_{1,\infty}$$

$$|b_1(q) - b_1(\tilde{q})| \leq \frac{c_1}{\beta_1}max(\frac{R}{\beta_1},1)|r(q) - r(\tilde{q})|_{1,\infty}$$

10

$$|b_2(q) - b_2(\tilde{q})| \le \frac{2c_1\ell R}{\beta_1^2} max(\frac{R\beta_2}{\beta_1^2}, 1)|r(q) - r(\tilde{q})|_{1,\infty}$$

and

$$|\frac{1}{r(q)} - \frac{1}{r(\tilde{q})}| \le \frac{1}{\beta_1^2}\|r(q) - r(\tilde{q})\|_{C(0,1)}.$$

Applying these inequalities into (2.32), we have

$$|\sigma(q)(\phi, \psi) - \sigma(\tilde{q})(\phi, \psi)| \le K_8 |r(q) - r(\tilde{q})|_{1,\infty} |\phi|_V |\psi|_V \qquad (2.33)$$

where

$$K_8 = \frac{2c_1\ell}{\beta_1} max(\frac{R}{\beta_1}, 1) + \frac{2c_1\ell^2 R}{\beta_1^2} max(\frac{2R\beta_2}{\beta_1^2}, 1) + \frac{c_1}{\beta_1} max(\frac{R}{\beta_1}, 1) + \frac{2c_1\ell R}{\beta_1^2} max(\frac{R\beta_2}{\beta_1^2}, 1) + \frac{\ell h}{\beta_1^2}\gamma(\tilde{G}).$$

From the hypotheses (H-4), we can thus infer the continuity of the sesquilinear form $\sigma(q)(\cdot, \cdot)$ with respect to the parameter q in Q. The proof has been completed.

For the system (2.7), the output can be represented as the restriction of $\tilde{u}(t)$ to a subset $\Sigma \subset \partial G_1$ of positive measure, i.e,

$$y(t, q) = \tilde{u}(t, q)|_\Sigma. \qquad (2.34)$$

We assume (see (H-0)) throughout that the admissible parameter set Q is a given compact subset of R^n. The fundamental identification problem considered here is based on the fit-to-data functional (see [2]) given by

$$J(q) = \frac{1}{2} \int_0^{t_f} \|y(t, q) - y_d(t)\|_F^2 dt \qquad (2.35)$$

where $F = L^2(\Sigma)$, $\{y_d(t)\}_{t\epsilon T}$ are given observed data, and $y(t, q)$ is the solution of (2.7) corresponding to $q\epsilon Q$. Then our problem is stated as follows:

(IDP) Find $q^*\epsilon Q$ which minimizes $J(q)$ given in (2.35) subject to the system (2.7) and (2.34).

In the next section, we consider a family of approximating identification problems associated with (IDP).

11

III. APPROXIMATE IDENTIFICATION PROBLEMS

The approximation scheme we have employed is based on the use of a finite element Galerkin approach to construct a sequence of finite dimensional approximating identification problems. Let us choose $\bigcup_{N=1}^{\infty} \{\phi_i^N\}_{i=1}^N$ as a set of basis functions in $H^1(\tilde{G})$. That is, for all N, $\{\phi_i^N\}_{i=1}^N$ are linearly independent and $\bigcup_N span\{\phi_i^N\}_{i=1}^N$ is dense in the V norm in $V = H^1(\tilde{G})$. We choose the approximation subspaces as

$$H^N := span\{\phi_1^N, \phi_2^N, \cdots, \phi_N^N\}.$$

Then, we can define the approximate solution of Eq. (2.7) by

$$\tilde{u}^N(t,q) = \sum_{i \leq N} w_i^N(t,q)\phi_i^N \tag{3.1}$$

where $w_i^N(t,q)$ are chosen such that for $j = 1, 2, \cdots, N$,

$$< \frac{d\tilde{u}^N(t,q)}{dt}, \phi_j^N > + \sigma(q)(\tilde{u}^N(t,q), \phi_j^N) = L(t,q)(\phi_j^N) \tag{3.2a}$$

and

$$\tilde{u}^N(0) = \sum_{i \leq N} < \overline{u}_0 \circ \mathcal{T}^{-1}(q), \phi_i^N > \phi_i^N. \tag{3.2b}$$

Hence the system (2.7) and the output (2.34) can be approximated by solving the system

$$C^N \dot{w}^N(t,q) + A^N(q)w^N(t,q) = F^N(t,q) \tag{3.3a}$$

$$w^N(0) = \overline{w}_0^N \tag{3.3b}$$

$$y^N(t,q) = \sum_{i \leq N} w_i^N(t,q)[\phi_i^N]_\Sigma \tag{3.4}$$

where

$$[C^N]_{i,j} := < \phi_i^N, \phi_j^N > \qquad \text{for} \qquad i, j = 1, 2, \cdots, N$$

$$[A^N(q)]_{i,j} := \sigma(q)(\phi_j^N, \phi_i^N) \qquad \text{for} \qquad i, j = 1, 2, \cdots, N$$

$$[w^N(t,q)]_i := w_i^N(t,q) \qquad \text{for} \qquad i = 1, 2, \cdots, N$$

$$[F^N(t,q)]_i := L(t,q)(\phi_i^N) \qquad \text{for} \qquad i = 1, 2, \cdots, N$$

12

$$[w_0^N]_i := < \overline{u}_0 \circ \mathcal{T}^{-1}(q), \phi_i^N > \qquad \text{for} \qquad i = 1, 2, \cdots, N.$$

The approximating identification problems thus take the following form:

$(AIDP)^N$ Find $\hat{q}^N \epsilon Q$ which minimizes

$$J^N(q) = \frac{1}{2} \int_0^{t_f} \|y^N(t, q) - y_d(t)\|_F^2 dt \tag{3.5}$$

subject to the approximating system (3.3) and (3.4).

Our convergence results for the finite element schemes are summarized in the following two theorems.

Theorem 2: *Let $\{q^M\} \subset Q$ be a sequence such that $q^M \to q \epsilon Q$ as $M \to \infty$ and let $\tilde{u}^N(q^M)$ and $\tilde{u}(q)$ be the solutions of Eqs. (3.3) and (2.7) corresponding to q^M and q, respectively. Then, under hypotheses (H-0) to (H-6), we have $\tilde{u}^N(q^M) \to \tilde{u}(q)$ strongly in $L^2(T; H^1(\tilde{G}))$ as $N, M \to \infty$.*

Theorem 3: *Let $\hat{q}^N$ be a solution of the problem $(AIDP)^N$. Then the sequence $\{\hat{q}^N\}$ admits a convergent subsequence $\{\hat{q}^{N_k}\}$ with $\hat{q}^{N_k} \to \hat{q}$ as $k \to \infty$. Moreover, $\hat{q}$ is a solution of the problem* (IDP).

The proof of Theorem 2 follows from the general convergence framework for parameter identification problems given in [3] and [4]. To ensure the desired convergence, it suffices to show that the sesquilinear form $\sigma(q)(\cdot, \cdot)$ satisfies the continuity, coercivity and boundedness conditions as stated in [3], [4]. But this is a result of Theorem 1 under the hypotheses (H-0) to (H-4).

The proof of Theorem 3 can be carried out by using Theorem 2 and the compactness of Q. Since $\hat{q}^N$ is a solution of the problem $(AIDP)^N$, it is clear that

$$J^N(\hat{q}^N) \leq J^N(q) \qquad \text{for} \qquad \forall q \epsilon Q. \tag{3.6}$$

Thus, if we can argue that for any $q^M \to q$ in Q,

$$y^N(q^M) \to y(q) \qquad \text{in } L^2(T; F) \qquad \text{as} \qquad N, M \to \infty,$$

13

then, we can obtain the desired inequality

$$J(\hat{q}) \leq J(q) \qquad \text{for} \qquad \forall q \epsilon Q$$

by taking limits in (3.6). But the needed arguments follow immediately from Theorem 2 since

$$\|y^N(\hat{q}^{N_k}) - y(\hat{q})\|^2_{L^2(T;F)} \leq K\|\tilde{u}^N(\hat{q}^{N_k}) - \tilde{u}(\hat{q})\|^2_{L^2(T;V)}$$

where K is independent of $\hat{q}^{N_k}$ and $\hat{q}$.

IV. OPTIMIZATION TECHNIQUES FOR THE APPROXIMATE ESTIMATION PROBLEMS

Let $\hat{q}^N$ be an optimal solution of the problem $(AIDP)^N$. Then a necessary condition for $\hat{q}^N$ to be optimal is characterized by

$$\nabla_q J^N(\hat{q}^N) \cdot (q - \hat{q}^N) \geq 0 \qquad \text{for} \qquad \forall q \epsilon Q \tag{4.1}$$

where ∇_q denotes the gradient of $J^N(q)$ with respect to q. From Eq. (3.5), we have for $k = 1, 2, \cdots, n$

$$[\nabla_q J^N(q)]_k = \int_0^{t_f} (w_{q_k}^N(t,q))'(C_b^N w^N(t,q) - Y_d^N(t))dt$$

where

$$w_{q_k}^N = \nabla_{q_k} w^N(t,q)$$

$$[C_b^N]_{i,j} = <\phi_i^N, \phi_j^N>_F \qquad \text{for} \qquad i,j = 1,2,\cdots,N$$

$$[Y_d^N(t)]_j = <y_d(t), \phi_j^N>_F \qquad \text{for} \qquad j = 1,2,\cdots,N.$$

Using the same procedure as in [9], we can evaluate the gradient vector by (for $k = 1, 2, \cdots, n$)

$$[\nabla_q J^N(q)]_k = \int_0^{t_f} v^N(t,q)'\{[\nabla_{q_k} A^N(q)]w^N(t,q) - \nabla_{q_k} F^N(t,q)\}dt \tag{4.2}$$

where $v^N(t,q)$ is the solution of the adjoint equation,

$$-C^N \dot{v}^N(t,q) + A^{*N}(q)v^N(t,q) = Y_d^N(t) - C_b^N w^N(t,q) \tag{4.3a}$$

14

$$v^N(t_f, q) = 0. \tag{4.3b}$$

In Eq. (4.3a), the matrix $A^{*N}(q)$ is given by

$$[A^{*N}(q)]_{ij} = \sigma^*(q)(\phi_i^N, \phi_j^N)$$

where $\sigma^*(q)(\cdot, \cdot)$ is the adjoint sesquilinear form of $\sigma(q)(\cdot, \cdot)$ defined by

$$\sigma * (q)(\phi, \psi)$$

$$:= \int\int_{\tilde{G}} \left[\sum_{i,j \leq 2} a_{ij}(q, z) \frac{\partial \phi}{\partial z_j} \frac{\partial \psi}{\partial z_i} - \sum_{j \leq 2} b_j(q, z) \phi \frac{\partial \psi}{\partial z_j} + (c_0 - \sum_{j \leq 2} \frac{\partial b_j}{\partial z_j}(q, z)) \phi \psi \right] dz$$

$$+ \int_0^1 \frac{\ell h}{r(q, z_1)} [\phi\psi]_{\partial G_1} dz_1 + \int_0^\ell h[\phi\psi]_{\partial G_2 \cup \partial G_4} dz_2$$

$$+ \int_0^1 \frac{c_1 r'(q, z_1)}{r(q, z_1)} \{ \frac{\ell r'(q, z_1)}{r(q, z_1)} - 1 \} [\phi\psi]_{\partial G_3} dz_1$$

$$- \int_0^1 \frac{c_1 r'(q, z_1)}{r(q, z_1)} [\phi\psi]_{\partial G_1} dz_1.$$

Consequently, the optimality condition (4.1) of the problem $(AIDP)^N$ can be characterized by

$$\sum_{k=1}^n \int_0^{t_f} v^N(t, \hat{q}^N)' \{ [\nabla_{q_k} A^N(\hat{q}^N)] w^N(t, \hat{q}^N) - \nabla_{q_k} F^N(t, \hat{q}^N) \} (q_k - \hat{q}_k^N) \geq 0 \qquad \text{for all} \qquad q \epsilon Q. \tag{4.4}$$

In the sequel, we discuss computer implementation of numerical schemes for the problem $(AIDP)^N$. Since we can evaluate the gradient of the cost function using (4.2), many optimization techniques for the constrained problems are readily applicable to our problem (see [11] and the references therein). For ease in exposition, here the compact set $Q \subset R^N$ is assumed to be defined by

$$Q = \{ q = (q_1, q_2, \cdots, q_n) \epsilon R^N | \Pi q \leq \bar{q} \} \tag{4.5}$$

where Π and $\bar{q}$ denote a given constraint matrix and vector, respectively. For the numerical results reported in this paper, we used the gradient projection method [12] which is

15

a particularly useful technique for optimization problems with the linear inequality constraints such as those given in (4.5). We use this method as presented in [12]; the iterative algorithm for finding $\hat{q}^N$ can thus be stated as follows:

Step 0: Choose an initial value $q^{(0)}$ in Q and set $i = 0$.

Step 1: If $\Pi q^{(i)} < \bar{q}$ set

$$g^{(i)} = -\nabla_q J^N(q^{(i)})$$

and proceed to *Step 3*; otherwise, proceed to *Step 2*.

Step 2: Compute the current direction by

$$g^{(i)} = -\frac{P\nabla_q J^N(q^{(i)})}{|P\nabla_q J^N(q^{(i)})|}$$

where

$$P = I - \Pi_p'(\Pi_p\Pi_p')^{-1}\Pi_p$$

and Π_p includes the gradient of all currently active constraints associated with matrix Π. If $g^{(i)} \neq 0$, proceed to *Step 3*; otherwise, proceed to *Step 4*.

Step 3: Compute $\lambda_{min}^{(i)}$ satisfying

$$J^N(q^{(i)} + \lambda_{min}^{(i)}g^{(i)}) = \min_{\lambda \in [0, \hat{\lambda}]} J^N(q^{(i)} + \lambda g^{(i)})$$

where $\hat{\lambda}$ is the largest step that may be taken from $q^{(i)}$ along $g^{(i)}$ without violating any constraint. If $\lambda_{min}^{(i)} = \hat{\lambda}$, then add the new contraints to the matrix Π_p and proceed to *Step 4*; otherwise, the new approximation to the solution is given by

$$q^{(i+1)} = q^{(i)} + \lambda_{min}^{(i)}g^{(i)}.$$

Replace $i + 1$ by i and return to *Step 1*.

Step 4: Compute the vector $\theta(q)$ by

$$\theta(q^{(i)}) = -(\Pi_p\Pi_p')^{-1}\Pi_p\nabla_p J(q^{(i)}).$$

If all components of θ are nonnegative, then set

$$\hat{q}^N = q^{(i)}$$

and terminate the computation; otherwise, delete the column of Π_p corresponding to the smallest component of $\theta(q^{(i)})$, replace $i+1$ by i and return to *Step 1*.

V. NUMERICAL PROCEDURES

In a series of numerical experiments, we used a test example constructed as follows: We chose a function $r(q)$, generated the corresponding solution numerically, added random noise, and then used this as "data" for our inverse algorithm. The parameter function $r(\xi, q)$ to be identified is a piecewise cubic polynomial function (see [6] for more details). We denote the knot sequence for r by

$$0 = \tau_0^n < \tau_1^n < \cdots < \tau_n^n < \tau_{n+1}^n = 1$$

and the unknown function $r(\xi, q)$ is given by

$$
\begin{aligned}
r(\xi, \cdot) &= p_i^n(\xi) \\
&= a_{1,i} + a_{2,i}(\xi - \tau_i^n) + a_{3,i}(\xi - \tau_i^n)^2/2 + a_{4,i}(\xi - \tau_i^n)^3/6 \qquad (5.1) \\
&\quad \text{for } \tau_i^n \le \xi \le \tau_{i+1}^n \qquad i = 0, 1, \cdots, n.
\end{aligned}
$$

The unknown parameter vector $q = \{q_i\}_{i=1}^n$ is then given by

$$q_i = r(\tau_i) \qquad \text{for} \qquad i = 1, 2, \cdots, n. \qquad (5.2)$$

Further, we assume

$$p_0(0, q) = p_n(1, q) = \ell \qquad (5.3)$$

$$p_0'(0, q) = p_n'(1, q) = 0. \qquad (5.4)$$

Substituting (5.2), (5.3), and (5.4) into (5.1), the coefficients $\{a_{k,i}\}$ can be determined uniquely and $r(\xi, q)$ satisfies the hypotheses (H-1), (H-2), and (H-4). In order to guarantee the hypothesis (H-3), we impose the constraints

$$\beta_1 \le q_i \le \beta_2 \qquad \text{for} \qquad i = 1, 2, \cdots, n.$$

17

Hence, the matrix Π ($2n \times n$) and the vector $\overline{q}$ ($2n \times 1$) defining the admissible parameter class Q (see (4.5)) is given by

$$\Pi = \begin{bmatrix} 1 & & & \\ -1 & & & 0 \\ & 1 & & \\ & -1 & & \\ & & \ddots & \\ 0 & & & 1 \\ & & & -1 \end{bmatrix} \qquad \overline{q} = \begin{bmatrix} \beta_2 \\ -\beta_1 \\ \vdots \\ \beta_2 \\ -\beta_1 \end{bmatrix}.$$

To discretize the system model by the finite element method, the domain G is divided into a finite number of elements $\{e_k\}_{k=1}^{K}$ ($K \leq N$) and a number of nodes defined by $\{z_i = (z_1^i, z_2^i)\}_{i=1}^{N}$ are selected in $\tilde{G}$. For convenience of computations, we set $\ell = 1$ in $\tilde{G}$. Each element is preassigned as an axiparallel rectangle with nodes at the vertices. The restriction of ϕ_i^N to any element e_k is given by the bilinear polynomial form,

$$\phi_i^N(z) = c_{i,k}^{(1)} + c_{i,k}^{(2)} z_1 + c_{i,k}^{(3)} z_2 + c_{i,k}^{(4)} z_1 z_2 \tag{5.5}$$

for $z = (z_1, z_2) \epsilon e_k$ $\qquad k = 1, 2, \cdots, K$ $\qquad$ and $\qquad i = 1, 2, \cdots, N$.

The coefficients $\{c_{i,k}^{(j)}\}$ can be chosen such that each polynomial form (5.5) satisfies the properties of a piecewise bilinear basis function (see e.g., [1], Ch. 5). The integration of element matrices $C^N, A^N(q), A^{*N}(q)$, and C_b^N, and the element vectors F^N and Y_d^N can be computed numerically by a Gauss-Legendre formula. Thus, the state model (3.3) and its adjoint system (4.3) can be solved numerically by an implicit scheme with respect to discrete time $t = ih$ ($i = 0, 1, \cdots, m$) where $h = t_f/m$. The evaluation of cost functional J^N and its gradient $\nabla_q J^N$ is the computationally expensive part of our algorithm since these involve the integration of the states $w^N(t, q)$ and the adjoint states $v^N(t, q)$ with respect to time t over $\overline{T}$. This can be accomplished by using the two-point Gauss formula.

The input data are preassigned as

$$\overline{u}_0(z) = -10, \qquad \text{for } z \epsilon \tilde{G}$$

$$f(\xi) = 0, \qquad \text{for } \xi \epsilon \partial G_1.$$

The known parameters c_1, c_0, and h in Eq. (1.1) were set as

$$c_1 = 0.034, \quad c_2 = 0.001, \quad h = 0.1.$$

The observed data $\{y_d(t)\}$ were generated by solving the finite element model (3.3). The number of finite elements and nodes in the numerical experiments were set as $K = 256$ (= 16×16) and $N = 289$ (= 17×17), respectively. The final time and number of time divisions were taken as $t_f = 10$ and $m = 100$. Random noise at various levels from 0% to 50% was added to the numerical solution, thereby producing simulated noisy "data" for the algorithm. The set Σ relative to data acquisition was given by

$$\Sigma = \bigcup_{j=1}^{p} N_{x_j}$$

where N_{x_j} denotes a neighborhood of points x_j at ∂G_1, i.e.,

$$N_{x_j} = (x_j - \varepsilon, x_j + \varepsilon) \qquad \text{for} \qquad j = 1, 2, \cdots, p.$$

Using such data, the estimation algorithm given in Section 4 was tested.

Example 1: In this example, the dimension of unknown vector was taken as $n = 4$ and the knot sequence $\{\tau_i^n\}_{i=0}^{n+1}$ was given by

$$\tau_i^4 = i/5 \qquad \text{for} \qquad i = 1, 2, \cdots, 5.$$

The values of the true parameters were chosen as

$$q_i = r(\tau_i^4) = 0.8 \qquad \text{for} \qquad i = 1, 2, 3, 4.$$

The lower and upper bounds of the unknown parameter vector were taken as $\beta_1 = 0.3$ and $\beta_2 = 1.1$, respectively. The initial guesses for the parameters were given by

$$q_i^{(0)} = 1 \qquad \text{for} \qquad i = 1, 2, 3, 4.$$

The number of sensors was taken as $p = 9$. Table 1 shows the estimated parameter numerical results for the data with noise free, 5%, 10%, and 50% relative noise and Figure 5.1

shows the estimated parameter function $r(\xi, \hat{q}^N)$ and true function $r(\xi, q)$ which correspond to the estimated boundary shape and true boundary for the 10% noise case.

		$\hat{q}_1$	$\hat{q}_2$	$\hat{q}_3$	$\hat{q}_4$	$\frac{1}{4}\sum_{i\leq 4}|q_i - \hat{q}_i|^2$
True Value		0.800	0.800	0.800	0.800	
Initial Guess		1.000	1.000	1.000	1.000	
Noise Free	iteration 6	0.850	0.882	0.880	0.849	3.36×10^{-2}
	iteration 13	0.820	0.819	0.821	0.819	9.92×10^{-3}
	iteration 17	0.810	0.785	0.810	0.806	5.39×10^{-3}
5% Noise	iteration 6	0.851	0.879	0.878	0.844	3.25×10^{-2}
	iteration 13	0.828	0.821	0.818	0.820	1.09×10^{-2}
	iteration 17	0.815	0.797	0.791	0.814	5.61×10^{-3}
10% Noise	iteration 6	0.849	0.853	0.861	0.834	2.51×10^{-2}
	iteration 14	0.787	0.847	0.835	0.750	1.95×10^{-2}
	iteration 18	0.827	0.792	0.799	0.796	7.20×10^{-3}
50% Noise	iteration 7	0.922	0.820	0.748	0.808	3.36×10^{-2}
	iteration 15	0.902	0.793	0.772	0.886	3.40×10^{-2}
	iteration 19	0.813	0.783	0.727	0.794	1.90×10^{-2}

Table 5.1. True Value and Estimated Values in Example 1.

Example 2: We chose the same dimension of unknown parameter vector as in Example 1 and we also used the same knot sequence. In this example, however, the values of the true parameters were preassigned as

$$q_1 = q_4 = 0.9$$

and

$$q_2 = q_3 = 0.6,$$

respectively. The lower and upper bounds, initial guess of unknown vector, and number of sensors were given by the same values as in Example 1. Table 5.2 shows the numerical results obtained here for the various sets of noisy data. Figures 5.2 and 5.3 represent the estimated parameter function for the case of 20% and 50% noisy observation case.
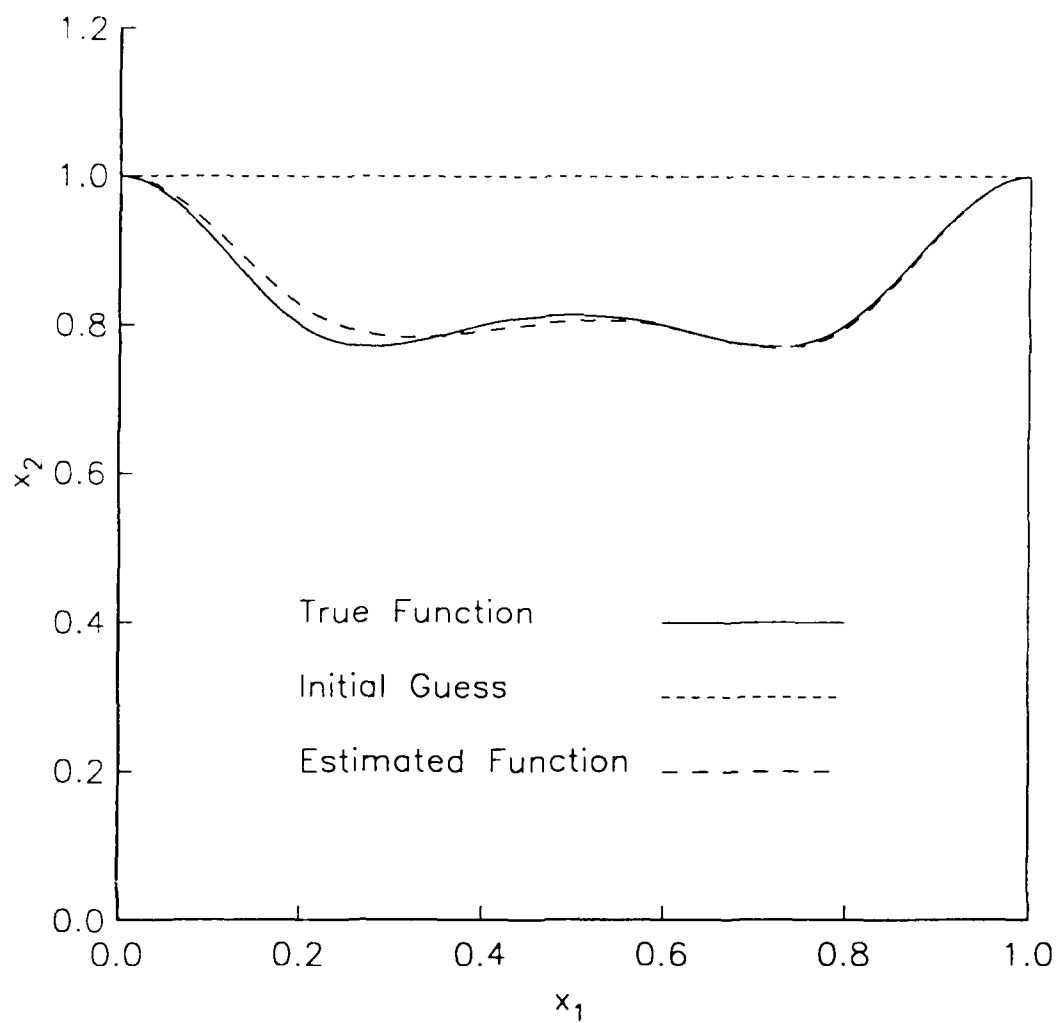
Figure 5.1. True Function and Estimated Function in Example 1 (10% Noise).

21

		$\hat{q}_1$	$\hat{q}_2$	$\hat{q}_3$	$\hat{q}_4$	$\frac{1}{4}\sum_{i\leq 4}|q_i - \hat{q}_i|^2$
	True Value	0.900	0.600	0.600	0.900	
	Initial Guess	1.000	1.000	1.000	1.000	
Noise	iteration 16	0.817	0.792	0.778	0.821	7.14×10^{-2}
Free	iteration 25	0.894	0.607	0.602	0.893	2.85×10^{-3}
5%	iteration 16	0.953	0.694	0.811	0.906	5.93×10^{-2}
Noise	iteration 26	0.896	0.604	0.605	0.898	1.93×10^{-3}
10%	iteration 16	0.902	0.807	0.674	0.949	5.62×10^{-2}
Noise	iteration 27	0.908	0.594	0.581	0.896	5.39×10^{-3}
20%	iteration 16	0.917	0.683	0.812	0.904	5.70×10^{-2}
Noise	iteration 27	0.902	0.603	0.610	0.887	4.19×10^{-3}
25%	iteration 16	0.939	0.819	0.684	0.962	6.15×10^{-2}
Noise	iteration 26	0.868	0.563	0.563	0.874	1.66×10^{-2}
50%	iteration 16	1.02	0.618	0.680	0.915	3.64×10^{-2}
Noise	iteration 28	0.951	0.574	0.599	0.953	1.95×10^{-2}

Table 5.2. True Value and Estimated Values in Example 2.

Example 3: In this example, we deal with a somewhat more difficult case as compared with Examples 1 and 2. We set the dimension of parameter space as $n = 8$ and we chose the knot sequence as

$$\{\tau_i^8\}_{i=0}^9 \qquad \tau_i^8 = i/9 \qquad \text{for } i = 0, 1, 2, \cdots, 9.$$

True parameter values were given by

$$q_1 = q_8 = 0.99,$$

$$q_2 = q_7 = 0.98,$$

$$q_3 = q_4 = 0.94,$$

and

$$q_5 = q_6 = 0.60,$$

respectively. Figure 5.4 shows the corresponding boundary shape to be identified. The number of sensors was taken as $p = 17$. The bounds and initial guesses for the parameter
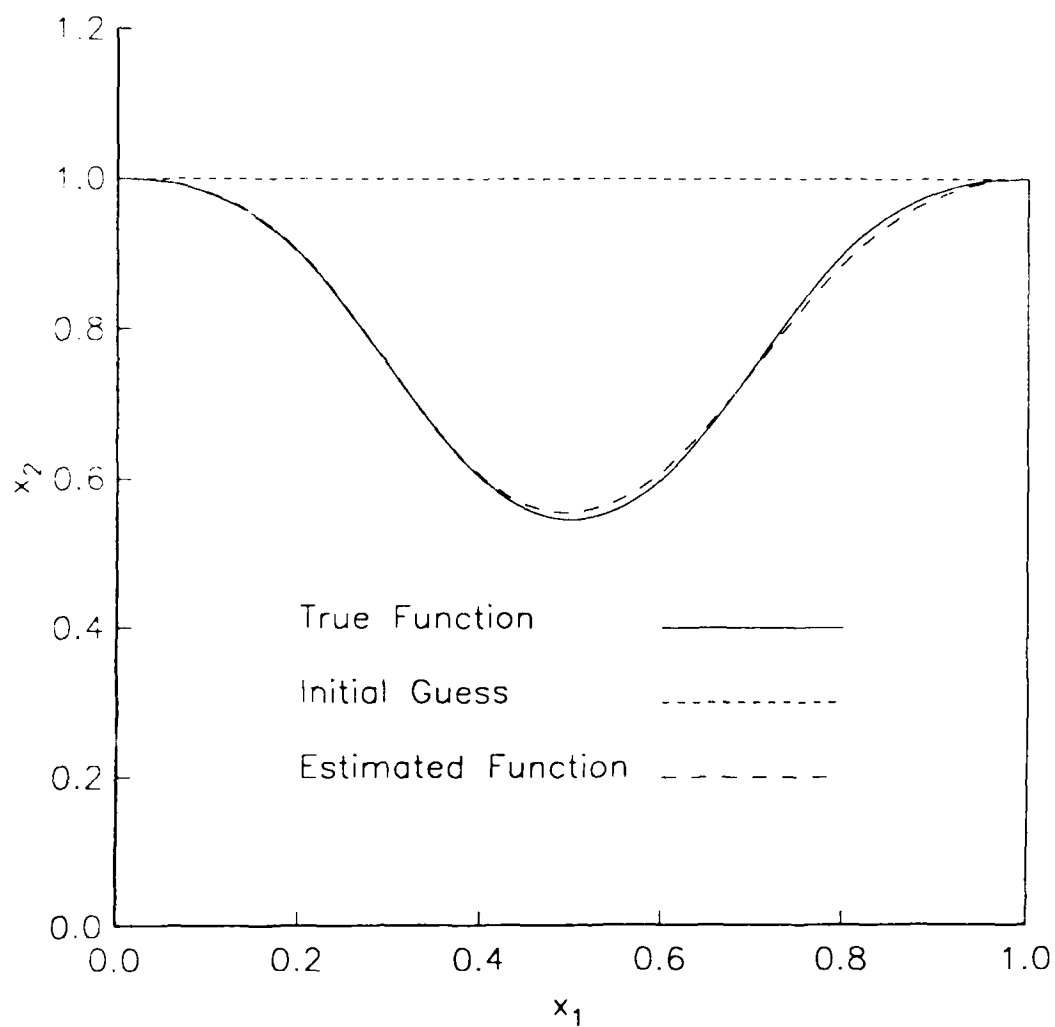
22

Figure 5.2. True Function and Estimated Function in Example 2 (20% Noise).
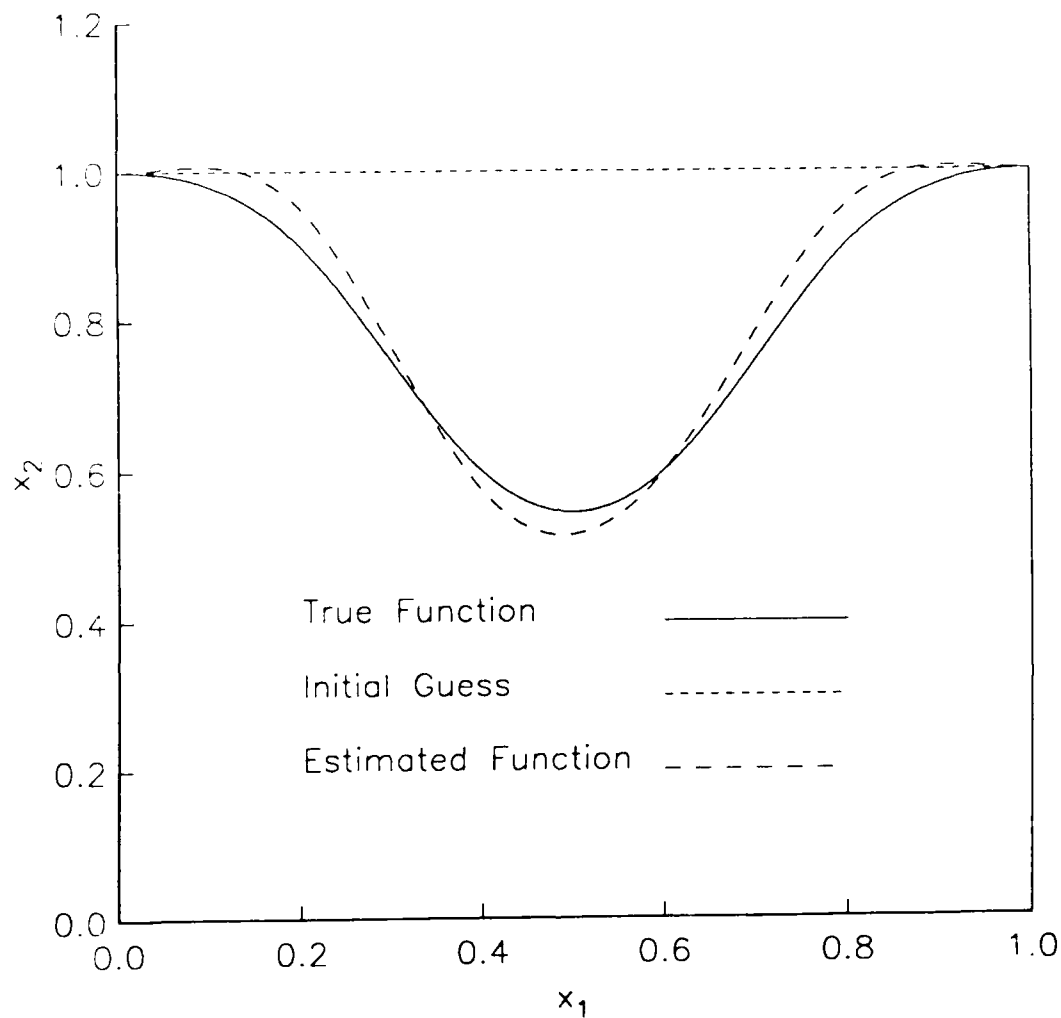
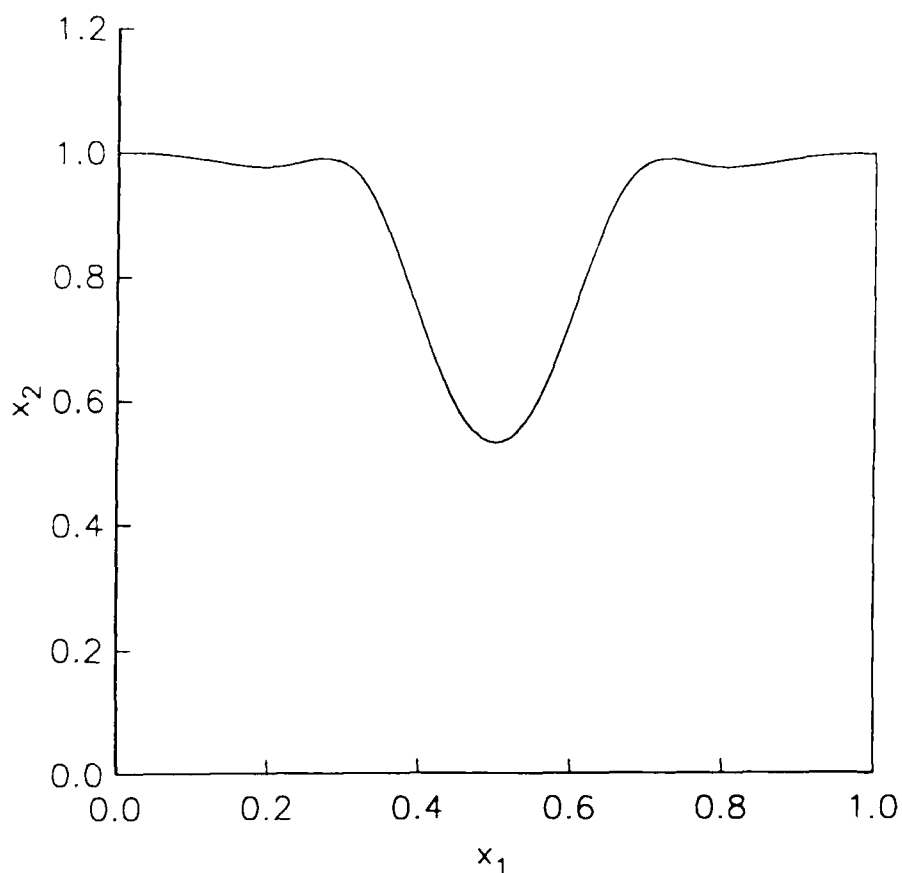Figure 5.3. True Function and Estimated Function in Example 2 (50% Noise).

Figure 5.4. Unknown boundary shape in Example 3.

vector were the same as in Examples 1 and 2. We ran numerical experiments for the case of noise free, 5%, 10%, 20%, and 50% noisy observations. Table 5.3 shows the estimated parameter vector obtained here. Figure 5.5 represents the estimated boundary curve for the 10% noisy data.

		$\hat{q}_1$	$\hat{q}_2$	$\hat{q}_3$	$\hat{q}_4$	$\hat{q}_5$	$\hat{q}_6$	$\hat{q}_7$	$\hat{q}_8$	$\frac{1}{8}\sum_{i\le 8}|q_i - \hat{q}_i|^2$
True Value		0.990	0.980	0.940	0.600	0.600	0.940	0.980	0.990	
Initial Guess		1.000	1.000	1.000	1.000	1.000	1.000	1.000	1.000	
Noise	iteration 16	1.039	1.027	0.887	0.808	0.674	0.926	1.029	1.033	3.08×10^{-2}
Free	iteration 23	1.014	1.007	0.943	0.624	0.615	0.943	1.003	1.017	7.27×10^{-3}
5%	iteration 16	1.042	1.031	0.879	0.749	0.666	0.920	1.049	1.031	2.85×10^{-2}
Noise	iteration 23	1.023	0.987	0.948	0.626	0.628	0.937	1.002	1.020	7.90×10^{-3}
10%	iteration 16	1.037	1.058	0.899	0.733	0.721	0.881	1.044	1.025	2.82×10^{-2}
Noise	iteration 24	1.010	1.009	0.955	0.586	0.578	0.948	0.994	1.000	6.20×10^{-3}
20%	iteration 16	1.034	0.989	0.950	0.592	0.595	0.994	1.018	1.061	1.61×10^{-2}
Noise	iteration 24	1.022	0.985	0.915	0.616	0.610	0.941	0.993	1.061	1.06×10^{-2}
50%	iteration 16	1.090	1.176	0.872	0.637	0.654	0.933	1.166	1.096	4.01×10^{-2}
Noise	iteration 24	1.030	1.033	0.939	0.566	0.603	0.933	1.046	1.052	1.47×10^{-2}

Table 5.3. True Value and Estimated Values in Example 3.

Throughout the numerical experiments, we checked the robustness of the algorithm with respect to noise in the observed data. Results in three examples indicated that the algorithm worked very well (i.e., as expected) for various noise levels. Furthermore, we checked the sensitivity of the algorithm with respect to the number of sensors. Specifically, we compared in Examples 2 and 3 the number of sensors (p) with the dimension of parameter space (n). In Example 2, for data with $p = 5 (> n = 4)$, the algorithm still yields an almost identical fit (to that for $p = 9$) even in 50% noise case while the fit could not be achieved under the reduced observation case $p = 3 (< n)$. Also, in Example 3, (where $n = 8$) the fit could not be obtained with $p = 3$ or $p = 5$, while the algorithm performed well with $p = 9$ $(> n)$. Carrying out a large number of other numerical tests in addition to those reported for Examples 2 and 3, we suggest that the algorithm requires a number of sensors which is at least equal to the number of dimensions of parameter space, i.e., $p \geq n$.

VI. CONCLUDING REMARKS

In this paper, we have discussed techniques for estimating the system boundary shape in two dimensional parabolic systems. By using a simple coordinate transformation technique, the parabolic PDE defined on unknown spatially varying domain was converted
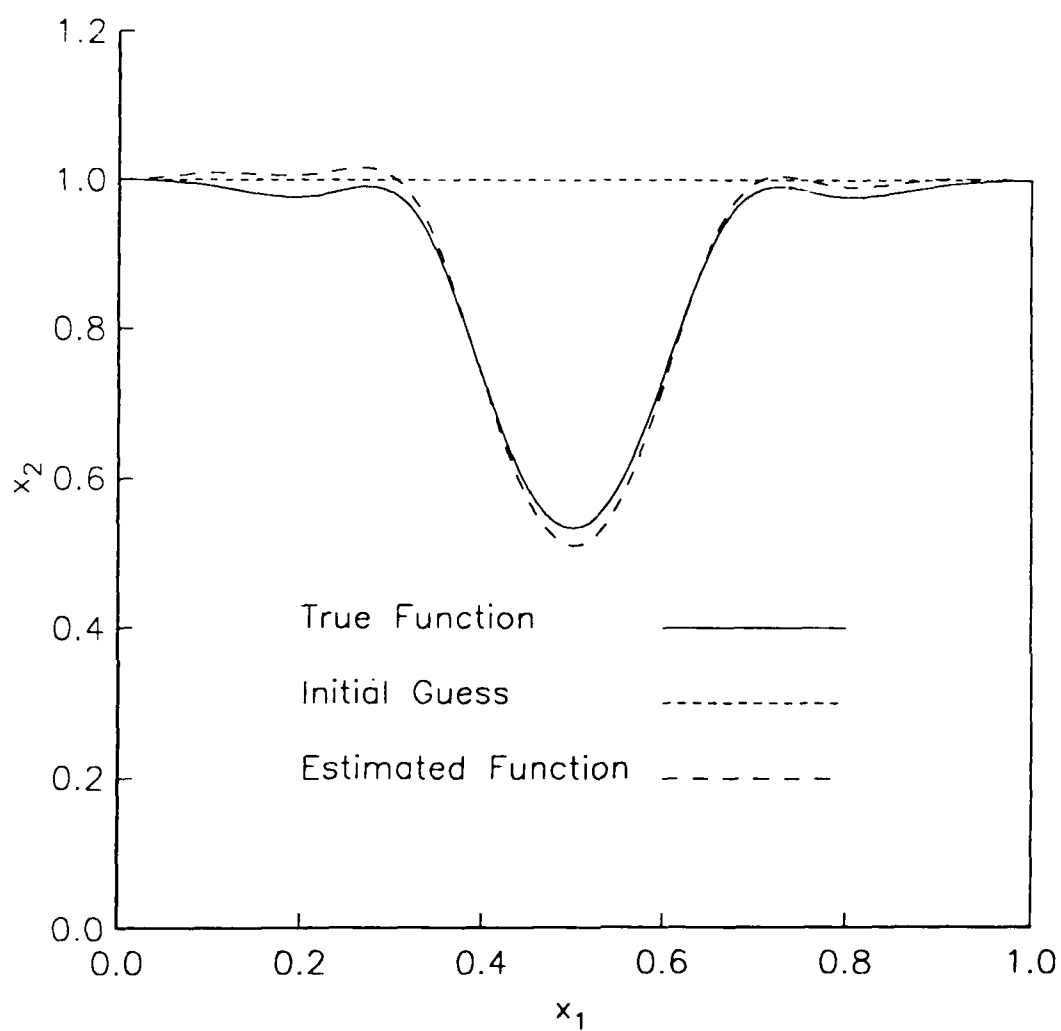
Figure 5.5. True Function and Estimated Function in Example 3 (10% Noise).

27

into the same type PDE with unknown coefficients defined on a fixed domain. Thus, our fundamental approach was placed within the theoretical framework for parameter identification problems given in [2],[3], and [4]. The practical utility of our algorithm is supported through a series of numerical experiments, a summary of which is given in Section 5. These simulations were carried out on the Sun Microsystems at ICASE, NASA Langley Research Center. For three different numerical examples, using data with no noise, the proposed algorithm yields an almost perfect fit, while, as expected, the fit degenerates significantly as noise in the observation becomes more pronounced.

Although here we discuss only the case where the unknown boundary shape is represented by a simple function of one variable, our basic parameter estimation ideas and techniques can be readily extended to consider more general classes of geometrical structures for the system boundary. For example, we may also treat the case where the unknown boundary shape is characterized by

$$r(q, x_1, x_2) = 0 \qquad \text{for} \qquad (x_1, x_2)\epsilon R^2.$$

We are currently pursuing investigations for these cases.

ACKNOWLEDGEMENT

References

[1] O. Axelsson and V. A. Barker, Finite Element Solution of Boundary Value Problems, Academic Press, New York, 1984.

[2] H. T. Banks, "On a variational approach to some parameter estimation problems," Distributed Parameter Systems, Lecture Notes in Control and Information Sciences, Vol. 75 (1985), pp. 1-23, Springer-Verlag, New York.

[3] H. T. Banks and K. Ito, "A theoretical framework for convergence and continuous dependence of estimates in inverse problems for distributed parameter systems," LCDS/CCS Report No. 87-20, Brown University, March 1987; Appl. Math. Lett., Vol. 0 (1987), pp. 31-35.

[4] H. T. Banks and K. Ito, "A unified framework for approximation in inverese problems for distributed parameter systems," LCDS/CCS Report No. 87-42, Brown University, October 1987; Control Theory Adv. Tech., to appear.

[5] D. Begis and R. Glowinski, "Application of the finite element method to the approximation of an optimum design problem," Appl. Math. Optim., Vol. 2 (1975), pp. 130-168.

[6] C. de Boor, A Practical Guide to Splines, Applied Mathematical Science, Vol. 27, Springer-Verlag, New York, 1978.

[7] D. Chenais, "On the existence of a solution in a domain identification problem," J. Math. Anal. Appl., Vol. 52 (1975), pp. 189-219.

[8] D. M. Heath, C. S. Welch, and W. P. Winfree, "Quantitative thermal diffusivity measurements of composites," in Review of Progress in Quantitative Nondestructive Evaluation, (D. G. Thompson and D. E. Chimenti, eds.), Plenum Publ., Vol. 5B (1986), pp. 1125-1132.

[9] J. L. Lions, <u>Optimal Control of Systems Governed by Partial Differential Equations</u>, Springer-Verlag, New York, 1971.

[10] O. Pironneau, <u>Optimal Shape Design for Elliptic Systems</u>, Springer-Verlag, New York, 1983.

[11] E. Polak, <u>Computational Methods in Optimization</u>, Academic Press, New York, 1971.

[12] J. B. Rosen, "The gradient projection method for nonlinear programming, Part I: Linear constraints," <u>SIAM J. Appl. Math.</u>, Vol. 8 (1960), pp. 181-217.

[13] J. Simon, "Differentiation with respect to the domain in boundary value problems," <u>Numer. Funct. Anal. Appl.</u>, Vol. 2 (1980), pp. 649-687.

[14] Y. Sunahara, Sh. Aihara, and F. Kojima, "A method for spatial domain identification of distributed parameter systems under noisy observations, <u>Proc. 9th IFAC World Congress, Budapest, Hungary, 1984</u>, Pergamon Press, New York, 1984.

[15] Y. Sunahara and F. Kojima, "Boundary identification for a two dimensional diffusion system under noisy observations," <u>Proc. 4th IFAC Symp. Control of Distributed Parameter Systems, UCLA, California, 1986</u>, Pergamon Press, New York, 1986.

Report Documentation Page

16. Abstract

This paper is concerned with the identification of the geometrical structure of the system boundary for a two-dimensional diffusion system. The domain identification problem treated here is converted into an optimization problem based on a fit-to-data criterion and theoretical convergence results for approximate identification techniques are discussed. Results of numerical experiments to demonstrate the efficacy of the theoretical ideas are reported.

END

DATED

FILM

8 — 88

DTIC